



# Infrared and Raman spectroscopic characterization of the carbonate mineral weloganite – $\text{Sr}_3\text{Na}_2\text{Zr}(\text{CO}_3)_6 \cdot 3\text{H}_2\text{O}$ and in comparison with selected carbonates

Ray L. Frost<sup>a,\*</sup>, Yunfei Xi<sup>a</sup>, Ricardo Scholz<sup>b</sup>, Fernanda Maria Belotti<sup>c</sup>, Mauro Cândido Filho<sup>d</sup>

<sup>a</sup> School of Chemistry, Physics and Mechanical Engineering, Science and Engineering Faculty, Queensland University of Technology, GPO Box 2434, Brisbane Queensland 4001, Australia

<sup>b</sup> Geology Department, School of Mines, Federal University of Ouro Preto, Campus Morro do Cruzeiro, Ouro Preto, MG 35,400-00, Brazil

<sup>c</sup> Federal University of Itajubá, Campus Itabira, Itabira, MG 35,903-087, Brazil

<sup>d</sup> Mining Engineer Department, School of Mines, Federal University of Ouro Preto, Campus Morro do Cruzeiro, Ouro Preto, MG 35,400-00, Brazil

## HIGHLIGHTS

- ▶ We have studied the mineral weloganite  $\text{Na}_2\text{Sr}_3\text{Zr}(\text{CO}_3)_6 \cdot 3\text{H}_2\text{O}$  using vibrational spectroscopy.
- ▶ Weloganite is member of the mckelveyite group, that includes donnayite-(Y) and mckelveyite-(Y).
- ▶ A comparison is made with the spectra of weloganite with other carbonate minerals.

## ARTICLE INFO

### Article history:

Received 13 December 2012

Received in revised form 5 February 2013

Accepted 5 February 2013

Available online 12 February 2013

### Keywords:

Raman spectroscopy

Weloganite

Carbonate

Infrared spectroscopy

Zirconium

## ABSTRACT

The mineral weloganite  $\text{Na}_2\text{Sr}_3\text{Zr}(\text{CO}_3)_6 \cdot 3\text{H}_2\text{O}$  has been studied by using vibrational spectroscopy and a comparison is made with the spectra of weloganite with other carbonate minerals. Weloganite is member of the mckelveyite group that includes donnayite-(Y) and mckelveyite-(Y).

The Raman spectrum of weloganite is characterized by an intense band at  $1082\text{ cm}^{-1}$  with shoulder bands at  $1061$  and  $1073\text{ cm}^{-1}$ , attributed to the  $\text{CO}_3^{2-}$  symmetric stretching vibration. The observation of three symmetric stretching vibrations is very unusual. The position of  $\text{CO}_3^{2-}$  symmetric stretching vibration varies with mineral composition. The Raman bands at  $1350$ ,  $1371$ ,  $1385$ ,  $1417$ ,  $1526$ ,  $1546$ , and  $1563\text{ cm}^{-1}$  are assigned to the  $\nu_3(\text{CO}_3)^{2-}$  antisymmetric stretching mode. The observation of additional Raman bands for the  $\nu_3$  modes for weloganite is significant in that it shows distortion of the carbonate anion in the mineral structure. The Raman band observed at  $870\text{ cm}^{-1}$  is assigned to the  $(\text{CO}_3)^{2-}$   $\nu_2$  bending mode. Raman bands observed for weloganite at  $679$ ,  $682$ ,  $696$ ,  $728$ ,  $736$ ,  $749$ , and  $762\text{ cm}^{-1}$  are assigned to the  $(\text{CO}_3)^{2-}$   $\nu_4$  bending modes. A comparison of the vibrational spectra is made with that of the rare earth carbonates decrespignyite, bastnasite, hydroxybastnasite, parisite, and northupite.

© 2013 Elsevier B.V. All rights reserved.

## 1. Introduction

The carbonates are a group of over 130 naturally occurring minerals containing the essential structural building block  $(\text{CO}_3)^{2-}$  [1]. Most of these minerals are relatively rare and quite often in association with other building blocks such as hydroxyls, halogens, sulfate, silicate, and phosphate.

Weloganite is a hydrated carbonate of Na, Sr and Zr. Its ideal chemical formula is given by  $\text{Na}_2\text{Sr}_3\text{Zr}(\text{CO}_3)_6 \cdot 3\text{H}_2\text{O}$  and belongs to triclinic system,  $P1$  or  $P-1$  space group, with cell parameters  $a = 8.988$ ,  $b = 8.988$ ,  $c = 6.730\text{ Å}$ ,  $\alpha = 102.84$ ,  $\beta = 116.42$ , and  $\gamma = 59.99^\circ$  [2]. The six carbonate groups and three water molecules in weloganite are linked together by six cations with the coordinations 10 (for the three  $\text{Sr}^{2+}$ ), 9 (for the  $\text{Zr}^{4+}$ ) and 6 (for the two  $\text{Na}^+$ ).

Each water molecule is hydrogen-bonded to two oxygens with average bond lengths of  $2.794\text{ Å}$  [3]. The mineral was described from St-Michel, Montreal Island, Quebec, Canada. It occurs in an alkalic sill, 5–10 feet thick, which has intruded Trenton (Ordovician) limestone [4,5]. Weloganite is member of the mckelveyite group, that includes donnayite-(Y) and mckelveyite-(Y) [6].

The Francon quarry consists of sequence of Ordovician-age limestone belonging to the Montréal Formation of the Trenton Group, and interbedded sills of alkaline sienite, monzonite, alkali olivine basalt and lamprophyre [8]. Weloganite crystals up to  $5.0\text{ cm}$  occur in miarolitic cavities. Other minerals in association are strontianite –  $\text{SrCO}_3$ , hydrodresserite –  $\text{BaAl}_2(\text{CO}_3)_2(\text{OH})_4 \cdot 3\text{H}_2\text{O}$ , cryolite  $\text{Na}_3\text{AlF}_6$ , calcite –  $\text{CaCO}_3$ , viitaniemiite –  $\text{Na}(\text{Ca},\text{Mn})\text{Al}(\text{PO}_4)(\text{F},\text{OH})_2(\text{OH})$ , siderite –  $\text{FeCO}_3$ , pyrrhotite –  $\text{Fe}_{1-x}\text{S}$ , molybdenite –  $\text{MoS}_2$ , mordenite –  $(\text{Na}_2,\text{Ca},\text{K}_2)_4[\text{Al}_8\text{Si}_{40}\text{O}_{96}] \cdot 28\text{H}_2\text{O}$ , barite –  $\text{BaSO}_4$ , celestine –  $\text{SrSO}_4$ , and dolomite –  $\text{CaMg}(\text{CO}_3)_2$  among others.

\* Corresponding author. Tel.: +61 7 3138 2407; fax: +61 7 3138 1804.

E-mail address: [r.frost@qut.edu.au](mailto:r.frost@qut.edu.au) (R.L. Frost).

Weloganite is named in honor of **Sir William E. Logan**, first director of the Geological Survey of Canada, 1842–1869, who laid the foundation of Canadian knowledge in the geology of the area [4,5].

Studies concerning the mineralogy of weloganite mineral are rare in the literature and to the best knowledge of the authors, data about vibrational spectroscopic characterization are restricted to the database of the University of Arizona (rruff.info), however no interpretation is given. No Raman spectroscopic investigation of these carbonate phases related to the mckelveyite group has been published. However, in recent years, the application of spectroscopic techniques to understand the structure of secondary minerals has been increasing.

The objective of this paper is to report the vibrational spectroscopic study of a weloganite mineral and relate the spectra to the molecular chemistry and the crystal chemistry of this carbonate mineral. We have characterized weloganite using Raman and infrared spectroscopy, with support of scanning electron microscopy in the mineral characterization.

## 2. Experimental

### 2.1. Samples description and preparation

The weloganite sample studied in this work was obtained from the collection of the Geology Department of the Federal University of Ouro Preto, Minas Gerais, Brazil, with sample code SAA-135. The sample is from the type locality for the mineral, the Francon quarry, located in the midst of Montréal, Québec province, Canada [7].

The sample was gently crushed and the associated minerals were removed under a stereomicroscope Leica MZ4. Scanning electron microscopy (SEM) was applied to support the mineralogical characterization.

### 2.2. Scanning electron microscopy (SEM)

Experiments and analyses involving electron microscopy were performed in the Center of Microscopy of the Universidade Federal de Minas Gerais, Belo Horizonte, Minas Gerais, Brazil (<http://www.microscopia.ufmg.br>).

Weloganite single crystal up to 2 mm was coated with a 5 nm Au. Secondary Electron and Backscattering Electron images were obtained using a JEOL JSM-6360LV equipment. A qualitative and semi-quantitative chemical analysis in the EDS mode was performed with a ThermoNORAN spectrometer model Quest and was applied to support the mineral characterization.

### 2.3. Raman microprobe spectroscopy

Crystals of weloganite were placed on a polished metal surface on the stage of an Olympus BHSM microscope, which is equipped with 10 $\times$ , 20 $\times$ , and 50 $\times$  objectives. The microscope is part of a Renishaw 1000 Raman microscope system, which also includes a monochromator, a filter system and a CCD detector (1024 pixels). The Raman spectra were excited by a Spectra-Physics model 127 He–Ne laser producing highly polarized light at 633 nm and collected at a nominal resolution of 2 cm<sup>-1</sup> and a precision of  $\pm 1$  cm<sup>-1</sup> in the range between 200 and 4000 cm<sup>-1</sup>. Repeated acquisitions on the crystals using the highest magnification (50 $\times$ ) were accumulated to improve the signal to noise ratio of the spectra. Raman Spectra were calibrated using the 520.5 cm<sup>-1</sup> line of a silicon wafer. The Raman spectrum of at least 10 crystals was collected to ensure the consistency of the spectra.

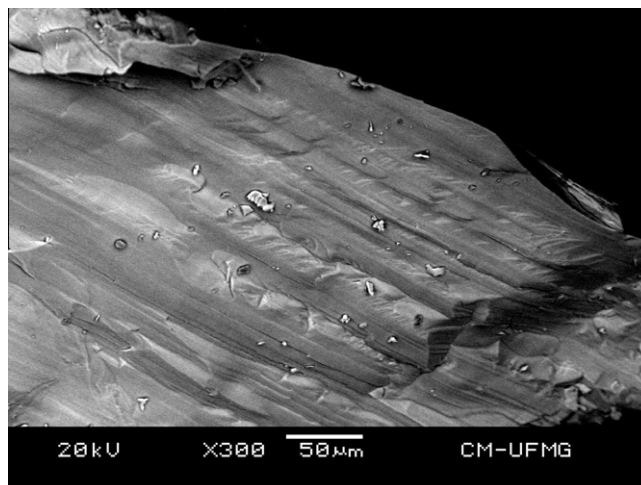


**Fig. 1.** Backscattered electron image (BSI) of a weloganite crystal up to 0.5 mm in length.

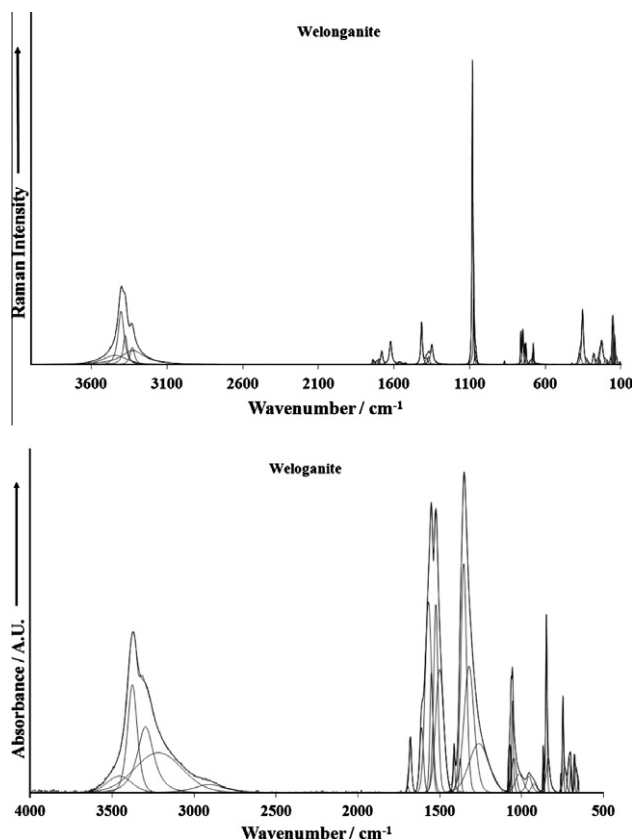


**Fig. 2.** (a) Raman spectrum of weloganite (upper spectrum) and (b) infrared spectrum of weloganite (lower spectrum).

### 2.4. Infrared spectroscopy

Infrared spectra were obtained using a Nicolet Nexus 870 FTIR spectrometer with a smart endurance single bounce diamond ATR cell. Spectra over the 4000–525 cm<sup>-1</sup> range were obtained by the co-addition of 128 scans with a resolution of 4 cm<sup>-1</sup> and a mirror velocity of 0.6329 cm/s. Spectra were co-added to improve the signal to noise ratio. The infrared spectra are given in the [Supplementary information](#).

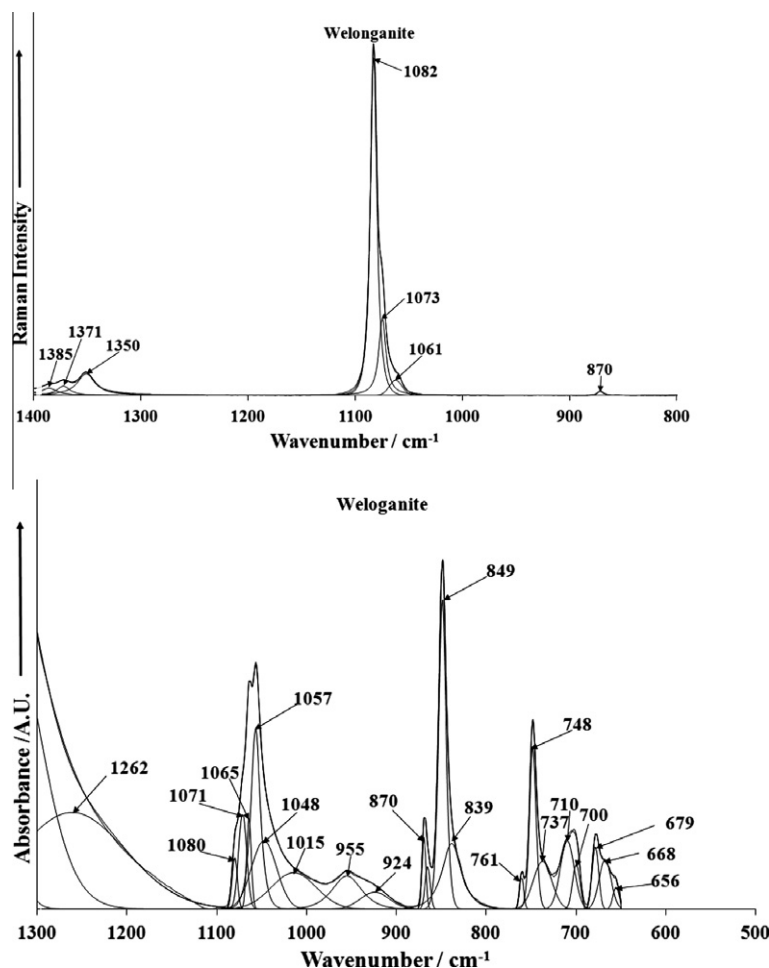


**Fig. 3.** (a) Raman spectrum of weloganite (upper spectrum) in the 800–1400 cm<sup>-1</sup> spectral range and (b) infrared spectrum of weloganite (lower spectrum) in the 500–1300 cm<sup>-1</sup> spectral range.

Spectral manipulation such as baseline correction/adjustment and smoothing were performed using the Spectralcalc software package GRAMS (Galactic Industries Corporation, NH, USA). Band component analysis was undertaken using the Jandel 'Peakfit' software package that enabled the type of fitting function to be selected and allows specific parameters to be fixed or varied accordingly. Band fitting was done using a Lorentzian–Gaussian cross-product function with the minimum number of component bands used for the fitting process. The Gaussian–Lorentzian ratio was maintained at values greater than 0.7 and fitting was undertaken until reproducible results were obtained with squared correlations of  $r^2$  greater than 0.995.

### 3. Results and discussion

#### 3.1. Chemical composition of weloganite

The SEM image of weloganite sample studied in this work is shown in Fig. 1. Weloganite single crystal shows a perfect cleavage along the {0001} plane. Qualitative chemical analysis shows a Sr, Zr and Na carbonate with minor amounts of Ca. The observed elements via SEM/EDS are in agreement with the chemical composition of weloganite.

#### 4. Spectroscopy of the carbonate anion

Nakamoto [9] first published and tabulated the selection rules for unidentate and bidentate anions including the carbonate anion.

The free ion, CO<sub>3</sub><sup>2-</sup> with D<sub>3h</sub> symmetry exhibits four normal vibrational modes; a symmetric stretching vibration ( $\nu_1$ ), an out-of-plane bend ( $\nu_2$ ), a doubly degenerate asymmetric stretch ( $\nu_3$ ) and another doubly degenerate bending mode ( $\nu_4$ ). The symmetries of these modes are A<sub>1</sub>' (R) + A<sub>1</sub>'' (IR) + E' (R, IR) + E'' (R, IR) and occur at 1063, 879, 1415 and 680 cm<sup>-1</sup> respectively. Generally, strong Raman modes appear around 1100 cm<sup>-1</sup> due to the symmetric stretching vibration ( $\nu_1$ ), of the carbonate groups, while intense IR and weak Raman peaks near 1400 cm<sup>-1</sup> are due to the antisymmetric stretch ( $\nu_3$ ). Infrared modes near 800 cm<sup>-1</sup> are derived from the out-of-plane bend ( $\nu_2$ ). Infrared and Raman modes around 700 cm<sup>-1</sup> region are due to the in-plane bending mode ( $\nu_4$ ). This mode is doubly degenerate for undistorted CO<sub>3</sub><sup>2-</sup> groups. As the carbonate groups become distorted from regular planar symmetry, this mode splits into two components. Infrared and Raman spectroscopy provide sensitive test for structural distortion of CO<sub>3</sub><sup>2-</sup>.

#### 5. Spectroscopy

The Raman spectrum of weloganite in the 100–4000 cm<sup>-1</sup> spectral range is displayed in Fig. 2a. This figure shows the position and relative intensities of the Raman bands. There are large parts of the spectrum where no intensity is observed and thus, the spectrum is divided into sections depending upon the type of vibration being studied. The infrared spectrum of weloganite over the 500–4000 cm<sup>-1</sup> spectral range is shown in Fig. 2b. Again, there are large parts of the spectrum where no intensity is observed, and

the spectrum may be subdivided into sections according to the type of vibration being examined.

The Raman spectrum of weloganite in the 800–1400  $\text{cm}^{-1}$  spectral range is displayed in Fig. 3a. The spectrum is dominated by a very intense sharp band at 1082  $\text{cm}^{-1}$  assigned to the  $\text{CO}_3^{2-}$   $\nu_1$  symmetric stretching mode. The main band has shoulders at 1073 and 1061  $\text{cm}^{-1}$ . Low intensity Raman bands are found at 1350, 1371 and 1385  $\text{cm}^{-1}$ . These bands are attributed to the  $\text{CO}_3^{2-}$   $\nu_3$  antisymmetric stretching modes. In the infrared spectrum shown in Fig. 3b, the  $\text{CO}_3^{2-}$   $\nu_1$  symmetric stretching mode is observed as a number of bands at 1057 and 1065  $\text{cm}^{-1}$  with shoulder bands at 1048, 1072 and 1080  $\text{cm}^{-1}$ .

A comparison may be made with other carbonate minerals. The symmetric stretching bands of carbonate for azurite and malachite were observed at 1090 and 1095  $\text{cm}^{-1}$ . Goldsmith and Ross report the infrared bending modes of carbonate at 837 and 817  $\text{cm}^{-1}$  for azurite and at 820 and 803  $\text{cm}^{-1}$  for malachite [10]. Two  $\nu_3$  modes were observed at 1490 and 1415  $\text{cm}^{-1}$  for azurite and at 1500 and 1400  $\text{cm}^{-1}$  for malachite. The observation of these two bands shows a loss of degeneracy. Such a conclusion is also supported by the observation of two  $\nu_4$  modes at 769 and 747  $\text{cm}^{-1}$  for azurite and 710 and 748  $\text{cm}^{-1}$  for malachite. The vibrational spectroscopy of these two minerals is complicated by this loss of degeneracy. Schmidt and Lutz report some vibrational spectroscopic data [11].

A further comparison may be made with some heavy metal carbonates. The Raman spectra of bastnasite are characterized by a single intense band at 1096  $\text{cm}^{-1}$  for the Pakistan mineral and 1085  $\text{cm}^{-1}$  for the mineral from Canada. The position of the band for the bastnasite from Norway is 1097  $\text{cm}^{-1}$ . The variation of the band position is a function of the chemical composition of the mineral. Farmer clearly shows the variation of the symmetric stretching mode as a function of the cation ionic radius [12]. Fundamentally the higher the ionic radius the lower the wavenumber of the symmetric stretching mode. It is proposed that the three symmetric stretching modes of the carbonate anion in the decrepignite structure are due to the presence of different adjacent cations. The Raman spectrum of parisite [13] shows two intense bands centered at 1088  $\text{cm}^{-1}$ . Evidence of splitting of this band is observed. Two bands are observed at 1086.5 and 1090.5  $\text{cm}^{-1}$ ; a result which is in agreement with the results for the infrared spectra of parisite where two bands at 1088 and 1078  $\text{cm}^{-1}$  were observed [14].

In the Raman spectrum a low intensity band at 870  $\text{cm}^{-1}$  is noted. This band is assigned to the  $\text{CO}_3^{2-}$   $\nu_4$  out-of-plane bending mode. This band shows much greater complexity in the infrared spectrum. Two distinct bands are observed at 849 and 868  $\text{cm}^{-1}$  with a shoulder band at 838  $\text{cm}^{-1}$ . A comparison of band positions may be compared with other heavy metal carbonates. The complexity of the carbonate symmetric stretching region of decrepignite-(Y) is reflected in the carbonate bending region. Four bands are observed at 791, 815, 837 and 849  $\text{cm}^{-1}$ . These bands are assigned to the  $(\text{CO}_3)^{2-}$   $\nu_2$  bending modes. In the infrared spectrum, bands are observed at 776, 787 and 800  $\text{cm}^{-1}$ . Wallwork et al. [15] also observed complexity in this spectral region; however no bands were defined or assigned. In contrast the Raman band for bastnasite is asymmetric and two bands may be resolved at 865 and 845  $\text{cm}^{-1}$ . For the mineral hydroxybastnasite, the symmetry is reduced and two low intensity bands are observed at 798 and 779  $\text{cm}^{-1}$ . The  $\nu_2$  bending mode is readily observed at 873  $\text{cm}^{-1}$  for the parisite mineral sample. In contrast, parisite mineral samples two distinct bands are observed at around 866 and 844  $\text{cm}^{-1}$ . For the mineral northupite a single very intense Raman band at 879  $\text{cm}^{-1}$  is observed. This band position is in excellent agreement with that reported by Adler and Kerr [14]. One conclusion that can be made is that the observation of one or more bend-

ing modes depends on the chemical composition of the halogenated carbonate.

The Raman spectrum in the 300–800  $\text{cm}^{-1}$  spectral range is displayed in Fig. 4a. A series of Raman bands are observed between 650 and 780  $\text{cm}^{-1}$ . Raman bands are observed at 679, 682, 696, 728, 736, 749, and 762  $\text{cm}^{-1}$ . These bands are all attributed to the  $\text{CO}_3^{2-}$   $\nu_2$  in-plane bending mode. In the infrared spectrum (Fig. 4b), an equivalent series of bands at 655, 668, 679, 699, 706, 718, 748, and 761  $\text{cm}^{-1}$  are assigned to the  $\text{CO}_3^{2-}$   $\nu_2$  in-plane bending modes.

Raman bands are observed for decrepignite at 694, 718 and 746  $\text{cm}^{-1}$  and are assigned to the  $(\text{CO}_3)^{2-}$   $\nu_4$  bending modes. Infrared bands are observed at 645, 678, 692, 724, and 745  $\text{cm}^{-1}$  and are attributed to this vibrational mode. The Raman band observed at 729  $\text{cm}^{-1}$  for the bastnasite is assigned to the  $\nu_4$  bending mode. Farmer in his treatise shows that there is a relationship between the position of the  $\nu_4$  mode and the ionic radius of the cation in the carbonate structure [12]. The variation in the position of the  $\nu_4$  band reflects the composition of the bastnasite. Two bands are observed for hydroxybastnasite at 602 and 569  $\text{cm}^{-1}$ . Whether these bands are ascribable to the  $\nu_4$  mode is uncertain. For the parisite mineral multiple bands are observed in the  $\nu_4$  region. Bands are observed at 789, 736, 739 and 712  $\text{cm}^{-1}$ . In the Raman spectrum of bastnasite a very low intensity band is observed at 735 (Pakistan) and 719  $\text{cm}^{-1}$  (Canada). Two Raman bands are observed for the parisite mineral sample at 682 and 742  $\text{cm}^{-1}$ . In the infrared spectrum of northupite a low intensity band at 714  $\text{cm}^{-1}$  is observed. Adler and Kerr also determined a band at 711  $\text{cm}^{-1}$  for northupite [14]. This band is assigned to the  $\nu_4$  bending mode. A comparison of this spectral region may be made with other carbonate minerals. For rosasite a number of infrared bands

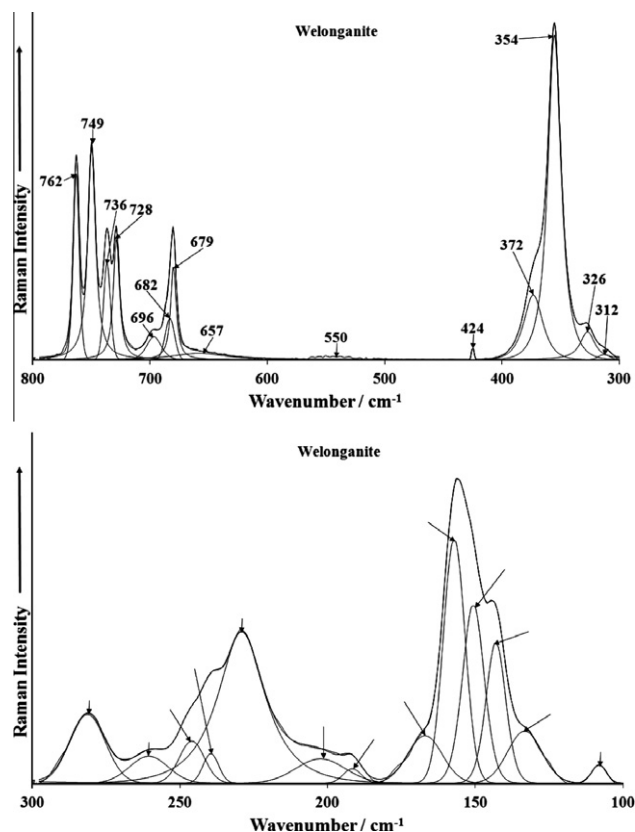


Fig. 4. (a) Raman spectrum of weloganite (upper spectrum) in the 300–800  $\text{cm}^{-1}$  spectral range and (b) Raman spectrum of weloganite (lower spectrum) in the 100–300  $\text{cm}^{-1}$  spectral range.

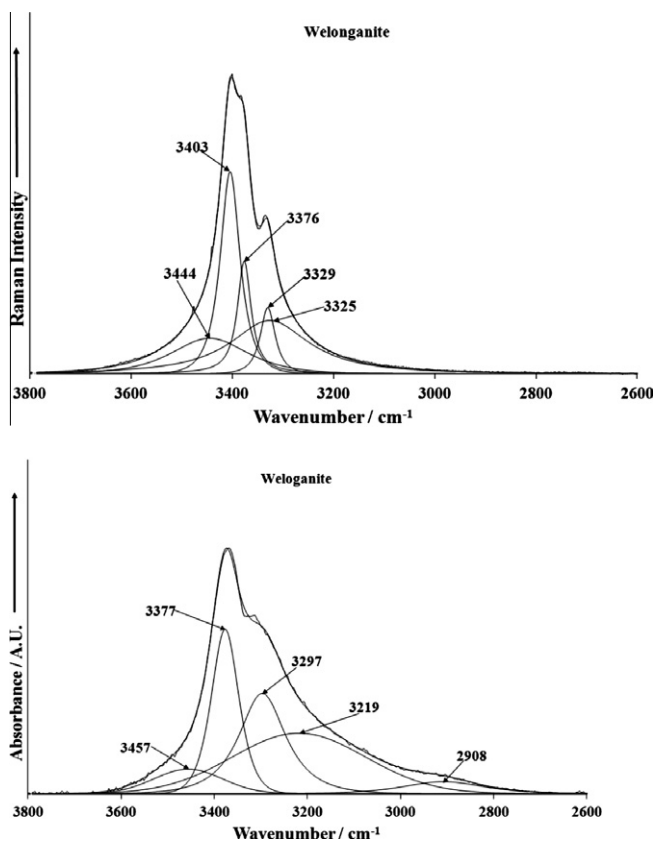


Fig. 5. (a) Raman spectrum of welonganite (upper spectrum) in the 2600–4000  $\text{cm}^{-1}$  spectral range and (b) infrared spectrum of welonganite (lower spectrum) in the 2600–4000  $\text{cm}^{-1}$  spectral range.

are observed at 776, 748 and 710  $\text{cm}^{-1}$ . These bands are assigned to the  $\nu_4(\text{CO}_3)^{2-}$  bending modes. In the Raman spectrum, bands are observed at 751 and 719  $\text{cm}^{-1}$ . For malachite two infrared bands are observed at 748 and 710  $\text{cm}^{-1}$  which are assigned to this  $\nu_4(\text{CO}_3)^{2-}$  bending vibration [16,17].

The broad Raman band at 550  $\text{cm}^{-1}$  may be ascribed to a water librational mode. The very intense broadish Raman band at 354  $\text{cm}^{-1}$  with shoulders at 326 and 372  $\text{cm}^{-1}$  are assigned to Zr–O stretching vibrations. The far low wavenumber region is displayed in Fig. 4b. Strong Raman bands are found at 142, 149, 156, 228, and 280  $\text{cm}^{-1}$ . These bands are ascribed to external vibrations.

The Raman spectrum of welonganite in the 2600–3800  $\text{cm}^{-1}$  is shown in Fig. 5a. Raman bands found at 3329, 3376 and 3403  $\text{cm}^{-1}$  are attributed to the water stretching bands. The infrared spectrum of welonganite in the 2600–3800  $\text{cm}^{-1}$  spectral range is reported in Fig. 5b. Infrared bands are observed at 2914, 3295 and 3377  $\text{cm}^{-1}$ . Again, these bands are attributed to water stretching vibrations. The observation of multiple bands in the Raman and infrared spectrum provides support for the concept that the water molecules in the welonganite structure are not equivalent.

The Raman spectrum of bastnasite displays bands in similar positions at 3651, 3620, 3526, 3355, 3276, 3169, and 3203  $\text{cm}^{-1}$ . The three higher wavenumber bands (3651, 3620, and 3526  $\text{cm}^{-1}$ ) are most likely assignable to OH stretching vibrations. Raman spectra of a Chinese bastnasite have been published but no spectral information is available for comparison in this spectral region [18]. Another study reported some Raman data for rare earth carbonates [19]. However no spectral information in the OH stretching region was reported. The Raman spectrum of the hydroxybastnasite shows several bands at 3741, 3535, 3430, 3352, and 3317  $\text{cm}^{-1}$ . For this mineral OH units replace F in a com-

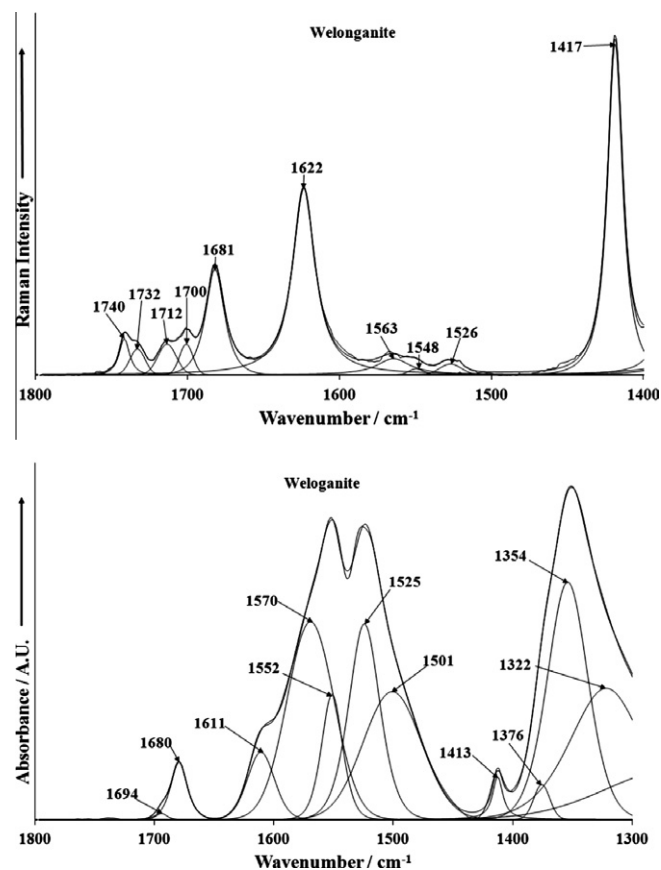


Fig. 6. (a) Raman spectrum of welonganite (upper spectrum) in the 1400–2000  $\text{cm}^{-1}$  spectral range and (b) infrared spectrum of welonganite (lower spectrum) in the 1300–1800  $\text{cm}^{-1}$  spectral range.

plex structure. It is possible that all of this set of bands is attributable to OH stretching vibrations. Aleksandrov described two types of bastnasites namely fluorobastnasite and hydroxybastnasite [20]. Another paper described the IR spectra in this spectral region with no detail except to state bands were observed [21]. For the mineral parasite broad bands in the OH stretching region are observed. Four Raman bands are observed at 3661, 3517, 3316 and 3180  $\text{cm}^{-1}$ .

The Raman spectrum of welonganite in the 1400–1800  $\text{cm}^{-1}$  spectral range is illustrated in Fig. 6a. The two Raman bands at 1622 and 1681  $\text{cm}^{-1}$  are attributed to water bending modes. The observation of two bending modes supports the concept of non-equivalent water molecules. The infrared spectrum in the 1300–1800  $\text{cm}^{-1}$  spectral range is reported in Fig. 6b. The series of infrared bands at 1322, 1354, 1376, 1413, 1502, 1524, 1552, and 1569  $\text{cm}^{-1}$  are all attributed to the  $\text{CO}_3^{2-}$   $\nu_3$  antisymmetric stretching modes. The Raman band at 1417  $\text{cm}^{-1}$  together with the low intensity Raman bands at 1526, 1548 and 1563  $\text{cm}^{-1}$  are assigned to the  $\text{CO}_3^{2-}$   $\nu_3$  antisymmetric stretching modes. The two infrared bands at 1611 and 1680  $\text{cm}^{-1}$  are attributed to water bending modes.

## 6. Conclusions

We have used vibrational spectroscopy to study aspects of the molecular structure of welonganite  $\text{Na}_2\text{Sr}_3\text{Zr}(\text{CO}_3)_6 \cdot 3\text{H}_2\text{O}$ . Welonganite is member of the mckelveyite group that includes donnayite-(Y) and mckelveyite-(Y). Multiple bands are observed in both the Raman and infrared spectra of welonganite providing evidence for the distortion of the carbonate anion in the welonganite structure, resulting in a loss of symmetry. This distortion is further

evidenced by the number of bands in the in-plane and out-of-plane bending regions. Multiple bands are observed in both the Raman and infrared spectra in the OH stretching region, proving that the water molecules are not equivalent in the weloganite structure.

### Acknowledgements

The financial and infra-structure support of the Discipline of Nanotechnology and Molecular Science, Science and Engineering Faculty of the Queensland University of Technology, is gratefully acknowledged. The Australian Research Council (ARC) is thanked for funding the instrumentation. The authors would like to acknowledge the Center of Microscopy at the Universidade Federal de Minas Gerais (<http://www.microscopia.ufmg.br>) for providing the equipment and technical support for experiments involving electron microscopy. R. Scholz thanks to FAPEMIG – Fundação de Amparo à Pesquisa do Estado de Minas Gerais (Grant No. CRA – APQ-03998-10).

### Appendix A. Supplementary material

Supplementary data associated with this article can be found, in the online version, at <http://dx.doi.org/10.1016/j.molstruc.2013.02.005>.

### References

- [1] P.A. Williams, Oxide Zone Geochemistry, Ellis Horwood Ltd., Chichester, West Sussex, England, 1990.
- [2] T.T. Chen, G.Y. Chao, *Canadian Mineralogist* 13 (Pt. 1) (1975) 22.
- [3] J.D. Grice, G. Perrault, *Canadian Mineralogist* 13 (Pt. 3) (1975) 209.
- [4] A.P. Sabina, Paper – Geological Survey of Canada 79-1A (1979) 115.
- [5] A.P. Sabina, J.L. Jambor, A.G. Plant, *Canadian Mineralogist* 9 (1968) 468.
- [6] M.E. Back, J.A. Mandarino, *Mineralogical Record* (2008).
- [7] P. Tarasoff, L. Horvath, E. Pfenninger-Horvath, *Mineralogical Record* 37 (2006) 5.
- [8] G.N. Eby, 22 (1985) 1103.
- [9] K. Nakamoto, *Infrared Spectra of Inorganic and Coordination Compounds*, 1963.
- [10] J.A. Goldsmith, S.D. Ross, *Spectrochimica Acta, Part A: Molecular and Biomolecular Spectroscopy* 24 (1968) 2131.
- [11] M. Schmidt, H.D. Lutz, *Physics and Chemistry of Minerals* 20 (1993) 27.
- [12] V.C. Farmer, *Mineralogical Society Monograph 4: The Infrared Spectra of Minerals*, 1974.
- [13] R.L. Frost, M.J. Dickfos, *Journal of Raman Spectroscopy* 38 (2007) 1516.
- [14] H.H. Adler, P.F. Kerr, *American Mineralogist* 48 (1963) 839.
- [15] K. Wallwork, U. Kolitsch, A. Pring, L. Nasdala, *Mineralogical Magazine* 66 (2002) 181.
- [16] R.L. Frost, W.N. Martens, L. Rintoul, E. Mahmutagic, J.T. Kloprogge, *Journal of Raman Spectroscopy* 33 (2002) 252.
- [17] R.L. Frost, Z. Ding, J.T. Kloprogge, W.N. Martens, *Thermochimica Acta* 390 (2002) 133.
- [18] H. Fan, K. Tao, Y. Xie, K. Wang, *Yanshi Xuebao* 19 (2003) 169.
- [19] W. Hong, S. He, S. Huang, Y. Wang, H. Hou, X. Zhu, *Guangpuxue Yu Guangpu Fenxi* 19 (1999) 546.
- [20] I.V. Aleksandrov, V.I. Ivanov, L.A. Sin'kova, *Zapiski Vserossiiskogo Mineralogicheskogo Obschestva* 94 (1965) 323.
- [21] Z. Maksimovic, G. Panto, *Mineralogical Magazine* 49 (1985) 717.